Electrical characterization of P_b centers in (100)Si–SiO_2 structures: The influence of surface potential on passivation during post metallization anneal

Lars-Åke Ragnarsson[a] and Per Lundgren
Microtechnology Centre at Chalmers and Solid State Electronics Laboratory, Department of Microelectronics, Chalmers University of Technology, SE-412 96 Göteborg, Sweden

(Received 8 November 1999; accepted for publication 15 February 2000)

Capacitance–voltage measurements were made on Cr-gated metal–oxide–silicon structures with ultrathin (~30 Å) thermal oxides. Using an empirical model, activation energies for the passivation of the P_b center were determined and found to be dependent on the charge state of the defect. Depassivation was found to occur at positive gate biases. © *2000 American Institute of Physics.* [S0021-8979(00)06810-9]

I. INTRODUCTION

One of the dominant imperfections at the Si–SiO_2 interface is a Si atom with a dangling bond—the P_b center. This defect exists on both ⟨100⟩ and ⟨111⟩ oriented substrates (although it is denoted P_{b0} on ⟨100⟩ oriented Si). It is electrically active and has two energy levels in the Si band gap, one at ~0.25 eV (above the valence band edge) where a single electron is trapped (+/0) and one at ~0.85 eV where a second electron is captured (0/−).[1] Its electrical activity is eliminated by a hydrogen atom[2–5] which shifts the energy levels out of the Si band gap thus passivating the defect.[1] The hydrogen passivation reactions of the P_b center

$$P_b + H_2 \rightarrow P_b H + H, \tag{1}$$

$$P_b + H \rightarrow P_b H, \tag{2}$$

have been studied extensively in Si–SiO_2 structures with thick oxides using electron paramagnetic resonance (EPR)[3–6] and capacitance voltage (C–V)[2–4] measurements both on ⟨100⟩ and ⟨111⟩ oriented Si. The results of these studies also hold for ultrathin oxides as studied in Al and poly-Si gated metal–oxide–silicon (MOS) structures.[7–9]

In addition, theoretical simulations by Edwards[1] predict that the passivation dynamics of reactions (1) and (2) and also the reverse depassivation reactions should be dependent on the charge state of the P_b center. The rate of passivation—in the presence of either atomic or molecular hydrogen—of positively/negatively charged P_b centers is predicted to be higher/lower than that of neutral ones. Edwards also predicted that the activation energy for depassivation should be lower for negatively charged P_b centers thus shifting the balance between passivation and depassivation to a different point of equilibrium.

Andersson *et al.*[10] were able to show that the rate of P_b passivation in Al-gated (111) Si MOS devices was influenced by the applied bias during post metallization anneal (PMA). This was verified in subsequent experiments[11] on Al-gated (100) Si MOS devices, from which it was concluded that the rate of passivation during PMA was independent of the oxide thickness. From these studies it was further concluded that neither oxide field, tunnel current nor electron concentration influence the passivation dynamics.

However, in the previous studies[10,11] accurate evaluation of the influence of bias during PMA was difficult because (1) the interface states in Al-gated MOS devices passivate too fast even at low temperatures which makes it difficult to resolve the difference between biased and nonbiased PMA; (2) the Al-gated MOS devices are affected by changes in the accumulation capacitance during PMA due to a reduction by Al of part of the SiO_2 to Al_2O_3.[12–15] This reduction reaction is also believed to reduce the density of interface states (D_{it})[14,16] simultaneously with the studied passivation by hydrogen; (3) the experimental setup makes fast ramping of the anneal temperature *with* applied bias difficult and the bias is therefore applied *after* ramping. This third point is particularly important when the influence of positive bias with respect to the metal gate which should increase the depassivation rate, is studied. A large fraction of the defects might be passivated during the initial temperature ramping and some of the depassivation effect may be reversed by the subsequent down-ramping *without* bias, which would obscure the effect of the positive bias.

For studies where the intrinsic quality of the oxide and the Si–SiO_2 interface are of interest, a suitable candidate for the gate material is Cr. Previous studies[9] where the annealing behavior of Al, Cr, Au, and poly-Si gated devices were compared showed that the D_{it} values of the Cr-gated devices were least affected by thermal treatment.

In addition to problems due to the gate material, there is the difficulty of determining the charge state of the defects at different biases and temperatures. For thick oxide devices and low biases a large fraction of the applied bias is lost across the oxide.[17] The position of the Fermi level at the surface is then a strong function of the temperature. In contrast, for ultrathin oxides and low biases the major part of the bias is lost across the substrate. A change in temperature then only affects the surface potential and not the position of the Fermi level. Ultrathin oxide devices based on substrates with

[a]Electronic mail: loke@ic.chalmers.se

different doping levels and/or doping types but otherwise the same are thus expected to behave similarly when annealed with equal biases.

In this study, by using Cr instead of Al as the gate metal in (100) Si MOS devices with ultrathin oxides, we are able to show that both passivation and depassivation are dependent on the charge state of the defects.

II. EXPERIMENTS

A. Device fabrication

MOS devices were fabricated from ⟨100⟩ oriented 3 in. silicon wafers of *n* and *p* type having a resistivity of 1–10 Ω cm. The wafers were oxidized to form a thick field oxide. Thereafter followed a lithography step where devices with areas ranging from 2×2 to 100×100 μm^2 were defined. After an RCA clean at 60 °C and a final dip in diluted (2%) HF the gate dielectric was thermally grown in a 2% O_2/N_2 mixture at 900 °C for 20 min. Finally, the top contact of the devices was formed by evaporation of Cr. The oxide thickness (approximately 29 Å) was obtained from $C-V$ measurements using the method of Maserjian.[13,18]

B. Post metallization anneal

PMA was carried out in air on a hot plate heated to temperatures ranging from 155 to 320 °C. The sample was put on a preheated surface; bias was applied for the desired time after which the sample was placed on a cold metal plate. On each chip one device was annealed with bias applied to the gate, while for reference three devices were annealed without bias. The anneal time for biased and nonbiased devices are slightly different due to the elapsed time (about 15 s) between when the sample was put on the heated surface and when the desired bias was applied.

C. Measurements

High-frequency $C-V$ measurements were made at room temperature at a frequency of 10 kHz using an HP 4284A LCR meter. The measurements, acquired after 100, 1000, 10 000, and in a few cases 100 000 s of anneal, were compared to measurements made prior to the first anneal cycle. A few samples were annealed without interruption in order to investigate the influence of the repeated heating and cooling. The difference between the two annealing methods was found to be negligible.

An estimate of the D_{it} was made by comparing the HF $C-V$ curve with a theoretical one. The method has been described elsewhere[10] and relies on the fact that a large fraction of the fast interface states follows the 10 kHz signal. The obtained values are thus underestimates of the actual D_{it}, a fact of little consequence in this study where only relative values are of interest. The initial peak D_{it} of the Cr devices was estimated at $(3.0\pm0.2)\times10^{12}$ $cm^{-2}eV^{-1}$ both at 0.2 and 0.9 eV above the valence band edge using data from measurements on *p*- and *n*-type devices.

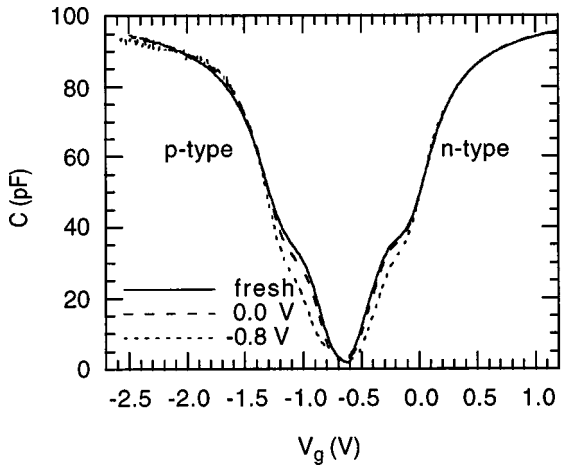

FIG. 1. High frequency $C-V$ curves (10 kHz) measured prior to and after a 10 000 s anneal at 170 °C on *p*- and *n*-type MOS devices.

III. RESULTS

A. Passivation dynamics of nonbiased and biased PMA

In Fig. 1 typical HF $C-V$ measurements acquired before and after a 10 000 s anneal at 170 °C on both *p*- and *n*-type devices are shown. Both types of devices show a clear difference between nonbiased (0.0 V) and biased (−0.8 V) anneal. There is also a difference between the two device types: the *p*-type device appears to anneal slightly faster than the *n*-type device. This is confirmed in Fig. 2 where the corresponding D_{it} values are shown. This unexpected difference in anneal rate can be explained by the fact that the $C-V$ curves of the *p*-type devices shift to more positive voltages during the PMA. The shift, which was estimated at 0.09 and 0.17 V for the nonbiased and −0.8 V cases, respectively, was subtracted from the *p*-type $C-V$ curves shown in Fig. 1 to show the impact of the anneal. A difference in the rate of passivation is thus to be expected since the effect of a positive voltage shift is equivalent to that of a negative shift of the bias. Therefore the PMA appears to occur at increasingly more negative biases. This has been shown to increase the anneal rate.[10] The consequence of this is that the fraction of

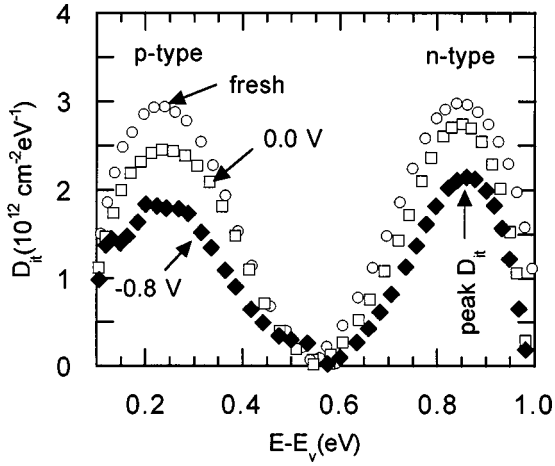

FIG. 2. The D_{it} of the devices in Fig. 1.

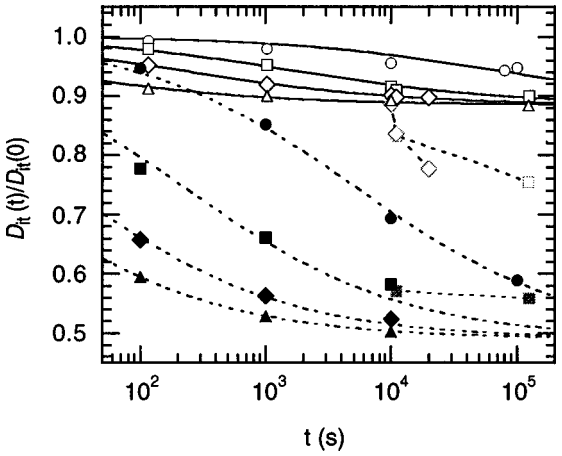

FIG. 3. The decrease of the relative peak D_{it} of normal (open symbols) and biased (−1.0 V) (closed symbols) anneal of Cr-gated *n*-type MOS devices. The temperature was 170 (○), 200 (□), 230 (◇), and 260 °C (△). Also shown is the biased passivation of previously nonbiased devices (◇, □) and the nonbiased passivation of a previously biased device (■).

defects that is positively charged varies with anneal time. This makes interpretation of the charge state impact on the PMA difficult for these *p*-type devices. Due to this difficulty the focus of the rest of the study is on *n*-type devices. It should be noted that the measured shifts stem only partially (<0.03 V) from the reduction of the D_{it}. The majority of the shift is a result of reduction of fixed charge in the oxide, apparently not present in the *n*-type devices.

In Fig. 3 the decrease of the relative peak D_{it} of *n*-type devices during anneal at temperatures ranging from 155 to 260 °C is shown. Also shown is the passivation dynamics during biased anneal at −1.0 V (filled symbols). A large difference between biased and nonbiased anneal is clearly seen in this figure. Furthermore, the decease *saturates* at a value depending slightly on the temperature and strongly on the anneal bias. This is in contrast to other studies of the passivation of P_b centers in nonmetal[4] and Al-gated[7,8,11] structures in which no saturation of the passivation was noted.

At temperatures above 260 °C, not shown here, the value of $D_{it}(t)/D_{it}(0)$ starts to increase immediately after a large but quick decrease. Whether this increase is an indication of depassivation or high temperature stress is not known and the data for these temperatures is therefore excluded. At biases below approximately −1.5 V the relative peak D_{it} also starts to increase, which is why this study was restricted to applied biases greater than −1.2 V.

To investigate the influence of temperature and bias on the saturation value, a few devices initially annealed without bias at 200 and 230 °C were given an extra anneal *with* bias at −1.0 V. The relative peak D_{it} of these devices is shown in Fig. 3. Although the value decreases with time, down to approximately 75% after 100 000 s, the decrease is substantially smaller than that of devices annealed with bias from the start. From this and the fact that the saturation level decreases with increasing negative bias during anneal (see Fig. 5), it appears that the hydrogen concentration at the surface is reduced not only by the passivation reaction but also by some other process. The lower saturation level at higher negative bias would then be due to more efficient usage of the initially higher concentration of hydrogen. However, the lower saturation values might also be explained by a reduction of the rate of depassivation which would shift the point of equilibrium towards a larger fraction of passivated P_b centers. In that case nonbiased anneal of a previously biased device would result in a higher saturation value. However, this is not what we observe: measurements on a device annealed first with an applied bias of −1.0 V for 10 000 s and then without bias for a further 123 000 s (see Fig. 3) resulted in a slightly decreased value of the peak D_{it}, close to that expected during continuously biased anneal. As a result it is necessary to combine these two processes—hydrogen consumption and depassivation rate reduction—to explain both the lower saturation level at negative biases and the depassivation occurring at positive biases.

B. Modeling the passivation dynamics

To analyze the impact of the bias on the passivation an empirical model according to

$$\frac{D_{it}(t)}{D_{it}(0)} = 1 - \alpha\left(1 - \frac{1}{1+\sqrt{k_a t}}\right), \tag{3}$$

was fitted to the passivation dynamics of the relative peak D_{it} at different temperatures and applied biases. The prefactors (k_{a0}) and the activation energies (E_a) of the rate constant

$$k_a = k_{a0} e^{-E_a/kT}, \tag{4}$$

were determined for three biases, 0.0, −0.5, and −1.0 V, while allowing α, the saturation value of the remaining unpassivated P_b centers, to vary freely. The values of α were found to have a negligible dependence on temperature but to depend exponentially on the activation energy as discussed below. The relation between applied bias and the approximate position of the Fermi levels ($E_{fs}-E_v$) at the surface was then calculated from a $C-V$ measurement using the Berglund integral.[19] In Fig. 4 the three determined E_a values are shown (large rectangles) as functions of the corresponding position of the Fermi level at the surface. Next, to calculate the activation energies at other biases a model for the relation between activation energy and $E_{fs}-E_v$ is needed.

If the passivation reactions of negative, neutral, and positive P_b centers have different activation energies, the single activation energy extracted from the passivation dynamics is an *effective* $E_{a,\mathrm{eff}}$ dependent on the fraction of charged and neutral P_b centers at a particular bias. Shown in Fig. 4 (dashed line) is $E_{a,\mathrm{eff}}$ averaged over the three extracted activation energies by weighting them by a Fermi–Dirac distribution of electrons at the surface and a Gaussian spread (0.1 eV) of the two transition levels. In Fig. 5 the decrease of the relative peak D_{it} as measured at 170 °C for different biases is shown together with calculated passivation dynamics using parameter values from Fig. 4. Worth noticing in Fig. 5 is the apparent grouping of the curves at different biases. In the bias ranges −0.2 to −0.6 and −1.0 to −1.2 V only small differences exist between the curves. This clustering around

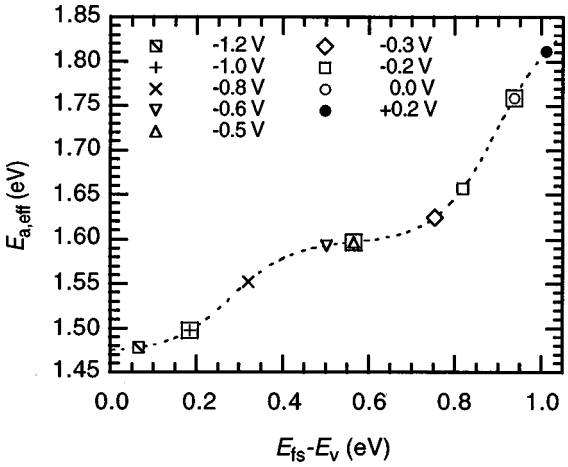

FIG. 4. Extracted activation energy for the passivation as a function of the approximate position of the Fermi level at the $Si-SiO_2$ interface. Large rectangles represent activation energies determined from measurements at different temperatures.

certain rate constants makes an $E_{a,\mathrm{eff}}$ relation other than the one shown in Fig. 4 improbable. For instance, a linear dependence on $E_{fs}-E_v$, is not appropriate. Instead, with values obtained from Fig. 4 a satisfactory fit to the data is achieved at all biases. However, at positive bias the peak D_{it} *increases*, presumably due to defect depassivation. The passivation of defects during nonbiased and negatively biased anneal is therefore also likely to be influenced by simultaneous depassivation, although at 170 °C the depassivation is expected to be very slow. Nevertheless, the consequence of this is a higher extracted $E_{a,\mathrm{eff}}$ than would be expected if the depassivation was negligible.

IV. DISCUSSION

A likely candidate for the competing hydrogen consuming process is the passivation of P_{b1} centers[4] which occurs in a manner analogous to that of P_{b0} passivation [reactions (1) and (2)]. The P_{b1} defect, present on (100) surfaces, was recently shown to be electrically inactive[20] and would consequently not be detected by the $C-V$ technique used in this study. Further, since the charge state of the P_{b1} center is independent of the position of the Fermi level at the surface (at least between the Si band edges) the passivation rate of P_{b1} centers is not expected to be sensitive to the bias. The large difference between the saturation levels for biased and nonbiased devices could thus be explained by the presence of P_{b1} centers that are equally ''slowly'' passivated at $V_A = -1.0$ V which results in a larger amount of hydrogen available for the passivation of P_{b0} centers. In this interpretation, to accurately model the passivation dynamics the initial concentrations of both defect types (P_{b0} and P_{b1}) and the amount of hydrogen (H and/or H_2) would have to be known.

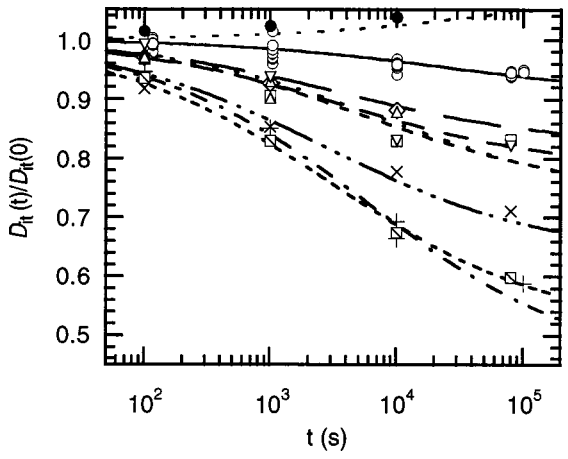

FIG. 5. Passivation dynamics of Cr-gated *n*-type MOS devices annealed at 170 °C with different biases. The symbols correspond to the ones used in Fig. 4.

There is also evidence of a standard deviation (σ_{Ea}) in the activation energy for the passivation reactions.[4] This spread is closely related to the spread in the (+/0) and (0/−) energy levels (here assumed to be Gaussian). It might further be related to local variations in the position of the Fermi level due to charges in the oxide and hence to a spread in the charge state of the defects. Therefore it is possible that the charge state of the defects can affect not only the activation energy but also σ_{Ea}. Stesmans[4] reported similar values of σ_{Ea} for P_{b0} and P_{b1} during nonbiased anneal. Due to the nonelectrical activity of the P_{b1} defect this similarity might not hold during biased anneal. Further studies are thus needed to determine the values of σ_{Ea} for the passivation of negatively and positively charged defects.

The possible complex interplay between the passivation reactions (1) and (2) of both P_{b0} and P_{b1} makes analytical modeling of the passivation dynamics very difficult. Since the focus of this study is to resolve the passivation bias dependence and not to accurately determine the concentrations of passivating agents, etc. the empirical approach was deemed sufficient. However, it is important to note that the activation energies determined from the passivation curves in Fig. 3 are obtained using an empirical function. Hence they are not expected to be equal to the activation energies of the actual reactions, but rather to represent the total passivation process. This makes the discrepancy between the activation energy found here for passivation of neutral P_b centers (1.60 eV) and that found by Stesmans (1.51 eV)[4] remarkably small. However, the important result is neither the values of the activation energies nor the empirical model, but that the activation energy of the passivation process, whether it be reaction (1), (2) or both, depends on the charge state of the P_b center.

V. CONCLUSIONS

In this study we see influences of applied bias during PMA on the passivation dynamics of the P_b defect. The activation energy of the passivation process was shown to be dependent on the position of the Fermi level at the $Si-SiO_2$ surface and hence the charge state of the P_b center. It was confirmed that if positively charged, the P_b defect is passivated more readily than if it is neutral or negative and further that depassivation is promoted by a negative charge state.

The passivation dynamics are predicted well using an empirical model, and the activation energies determined here.

ACKNOWLEDGMENTS

This work was partially sponsored by grants from the Swedish Research Council for Engineering Sciences and the Foundation for Strategic Research.

[1] A. Edwards, Phys. Rev. B **44**, 1832 (1991).
[2] M. L. Reed and J. D. Plummer, J. Appl. Phys. **63**, 5776 (1988).
[3] K. L. Brower, Appl. Phys. Lett. **53**, 508 (1988).
[4] A. Stesmans, Appl. Phys. Lett. **68**, 2076 (1996).
[5] E. Cartier, J. H. Stathis, and D. A. Buchanan, Appl. Phys. Lett. **63**, 1510 (1993).
[6] G. J. Gerardi, E. H. Poindexter, P. J. Caplan, and N. M. Johnson, Appl. Phys. Lett. **49**, 348 (1986).
[7] P. Lundgren and M. O. Anderson, J. Appl. Phys. **74**, 4780 (1993).
[8] M. O. Andersson, P. Lundgren, O. Engström, and K. R. Farmer, Microelectron. Eng. **22**, 235 (1993).
[9] P. Lundgren, J. Appl. Phys. **85**, 2229 (1999).
[10] M. O. Andersson, A. Lundgren, and P. Lundgren, Phys. Rev. B **50**, 11666 (1994).
[11] L.-Å. Ragnarsson, P. Lundgren, Z. Ovuka, and M. O. Anderson, J. Electrochem. Soc. **144**, 1866 (1997).
[12] R. S. Bauer, R. Z. Bachrach, and L. J. Brillson, Appl. Phys. Lett. **37**, 1006 (1980).
[13] M. H. Hecht, R. P. Vasquez, F. J. Grunthaner, N. Zamani, and J. Maserjian, J. Appl. Phys. **57**, 5256 (1985).
[14] R. McGrath, J. F. McGilp, I. T. McGovern, S. J. Morgan, W. G. Herrenden-Harker, and R. H. Williams, Semicond. Sci. Technol. **3**, 937 (1988).
[15] L.-Å. Ragnarsson, E. Aderstedt, and P. Lundgren, J. Electrochem. Soc. **146**, 2637 (1999).
[16] C. Anandan, Appl. Surf. Sci. **89**, 57 (1995).
[17] L.-Å. Ragnarsson and P. Lundgren, Microelectron. Eng. **48**, 219 (1999).
[18] J. Maserjian, G. Petersson, and C. Svensson, Solid-State Electron. **17**, 335 (1974).
[19] C. N. Berglund, IEEE Trans. Electron Devices **ED-13**, 701 (1966).
[20] A. Stesmans and V. V. Afanas'ev, Phys. Rev. B **57**, 10030 (1998).